electronics

MDPI

Article

Hybrid Feature Reduction Using *PCC*-Stacked Autoencoders for Gold/Oil Prices Forecasting under COVID-19 Pandemic

Nagwan Abdel Samee [1], Ghada Atteia [1], Reem Alkanhel [1,*], Amel Ali Alhussan [2] and Hussah Nasser AlEisa [2]

[1] Department of Information Technology, College of Computer and Information Sciences, Princess Nourah bint Abdulrahman University, P.O. Box 84428, Riyadh 11671, Saudi Arabia; nmabdelsamee@pnu.edu.sa (N.A.S.); geatteiaallah@pnu.edu.sa (G.A.)

[2] Department of Computer Sciences, College of Computer and Information Sciences, Princess Nourah bint Abdulrahman University, P.O. Box 84428, Riyadh 11671, Saudi Arabia; aaalhussan@pnu.edu.sa (A.A.A.); haleisa@pnu.edu.as (H.N.A.)

* Correspondence: rialkanhal@pnu.edu.sa; Tel.: +966-55-050-6818

Abstract: The financial markets have been influenced by the emerging spread of Coronavirus disease, COVID-19. The oil, and gold as well have experienced a downward trend due to the increased rate in the number of confirmed COVID-19 cases. Lately, the published COVID data comprised new variables that may influence the accuracy of the oil/gold prices forecasting models including the Stringency index, Reproduction rate, Positive Rate, and Vaccinations. In this study, Deep Autoencoders are introduced and combined with the well-known approach: Pearson Correlation Coefficient, *PCC*, analysis in selecting the key features that affect the accuracy of the forecasting models of gold and oil prices with respect to COVID-19 pandemic. We have utilized a hybrid approach of *PCC* along with a 2-Stage Stacked Autoencoder, SA, to extract the latent features which are then submitted to Neural Network, NN, regression model. The NN regressor has been trained using the Bayesian Regularization-backpropagation algorithm which provides a good generalization for small noisy datasets. The hybrid approach has yielded the minimum MSE values of 8.97×10^{-3} and 5.356×10^{-2} on the oil/gold validation set, respectively. Compared to the existing approaches, the proposed approach has outperformed the ARIMA, ML based regression models in forecasting the oil/gold prices. In addition, the introduced framework has yielded lower Mean Absolute Error, MAE, than the Recurrent Neural Network, RNN, and the Principal Component Analysis, PCA, for dimension reduction. The retrieved results showed that the hybrid method produced more robust features by considering the relationship between the input features.

Keywords: stacked autoencoders; neural network; forecasting models

Citation: Samee, N.A.; Atteia, G.; Alkanhel, R.; Alhussan, A.A.; AlEisa, H.N. Hybrid Feature Reduction Using *PCC*-Stacked Autoencoders for Gold/Oil Prices Forecasting under COVID-19 Pandemic. *Electronics* **2022**, *11*, 991. https://doi.org/10.3390/electronics11070991

Academic Editor: Grzegorz Dudek

Received: 15 February 2022
Accepted: 17 March 2022
Published: 23 March 2022

1. Introduction

Forecasting the prices of gold and oil has a great impact on the market participants, and portfolio risk management. Oil and gold are two important commodities for the global economy that are frequently included in equities portfolios of investors [1]. High uncertainty about the oil and gold prices may reduce the investments and increase investor worries, making portfolio risk management and asset allocation a big challenge for equity investors, traders, hedgers, and portfolio managers [2]. Oil prices are highly volatile, and the price fluctuations are a good predictor for forecasting commodities and financial asset prices. On the other hand, gold is often seen as a safe-haven asset during times of crisis [3]. Stockholders frequently switch between or bring together, oil and gold to vary their equity portfolios [4]. Lately, both commodities have been indicated by increasing instability and this has confused the investment decision-making. Therefore, accurate forecasting of the oil and gold prices may help the investors in taking their portfolio risk management decisions.

Once the COVID-19 pandemic occurred in China, the virus has been spread all over the world and it has significantly increased the uncertainty in the prices of the commodity markets including gold and oil [5]. The growth in the rate of mortality has forced the governments to enforce harsh restrictions including lockdowns and hold many business operations which have had serious consequences for economies and financial sectors [6]. As most of the economic activities have been halted during the lockdowns in approximately all industrialized economies, the price of the crude oil fell during 2020 and while the gold prices have taken an upward trend [7,8].

The existing methods for the forecasting of the oil and gold prices can be divided into two categories including spatial-based or historical-based prediction models [9]. From a spatial point of view, the forecasting model is constructed based on the factors that influence oil/gold prices. However, in the historical perspective, the construction is based on the historical values of the prices. Basically, the oil/gold prices have direct interactions among other market factors including the stock prices, and the US dollar [10]. As well as during the COVID-19 pandemic, the indirect impact of commodity markets has also affected the oil/gold prices. Therefore, spatial-based forecasting for oil/gold prices is the proper method during the COVID-19 pandemic.

Although the forecasting of the oil and gold prices during the Covid-19 pandemic is emerging, still few studies have been published in the literature in this regard. Mensi et al. [5] have investigated the price-switching spillovers between the stock, gold, and crude oil, futures prices before and during the global health crisis, COVID-19 pandemic. The parametric autoregressive technique has been employed to detect the connectedness between the stock, oil, and gold prices during the COVID-19. Dimitrios Bakas et al. [7] have empirically estimated the three 5-factor Vector Auto-Regressive, VAR, model for the instability of commodity markets including crude oil, broad commodity index, and gold.

Originally, there are various ML algorithms have been utilized for the forecasting of gold and crude oil prices. Such publications include classical ML regressors such as the ANN, SVM, and GPR [9,11–15] and Deep Learning algorithms [16–21]. Lately, ANNs have yielded outstanding performance in describing the nonlinear relationships among variables [22]. Moshiri and Foroutan [12] have set up a nonlinear ANN model for forecasting the crude oil prices from 1983 to 2003. The retrieved results using the ANN have surpassed the results yielded from the ARIMA, and GARCH regressors. Wang et al. [20] have utilized the filter and wrapper feature selection approaches to improve the retrieved performance of the ANN, and the SVM. Kristjanpoller and Minutolo [14] have proposed a hybrid frame including the ANN and GARCH in the prediction of crude oil and the composite model has yielded a better performance compared to the stand-alone ones. The overfitting of the ANN in forecasting the financial data has been resolved in [23] by introducing the Bayesian Regularization approach as a training algorithm. The deep learning-based forecasting models are based on time series analysis for the historical values of the gold and crude oil prices. The recurrent neural network, RNN, and the Long-term and Short-term Memory Model, LSTM, are deep learning approaches that consider the joint relationship of the long-term and short-term factors of crude oil, and gold prices [9].

The accuracy of the forecasting data model is greatly impacted by the significance of the input features [24]. Selecting the significant input features is accomplished using filter or wrapper methods. The *PCC* analysis is the dominant filter-based feature selection method for building forecasting models [25]. In the *PCC* analysis, the correlation coefficient between the outcome and input features is computed. Significant input features are those that are highly correlated with the response variable. Although the correlation-based feature selection is an early approach in building a forecasting data model, it does not ensure the dependency between the outcome and the selected input predictors. Instead, the multi-layer deep learning models such as Autoencoder [23] lately have yielded outstanding performance in extracting the latent deep features in the feature matrix [26].

In this study, we are introducing a hybrid approach including Deep Autoencoders, and Pearson correlation analysis in selecting the key features that affect the accuracy of

Crude oil and gold forecasting models during the COVID-19 pandemic. The retrieved significant features are used in the training and validation of an NN regressor which has lately yielded an outstanding performance in the forecasting of such commodities.

This research article paper is constructed as follows: a literature review is introduced in Section 2. The methods including the data exploration and its preprocessing, and the proposed *PCC*-Stacked Autoencoders model are explained in Section 3. Results are displayed and examined in Section 4. Lastly, the conclusion of the presented study is described in Section 5.

2. Literature Review

The data models for the prediction of gold and oil prices can be divided into two categories: empirical, and regression-based methods [27]. The main principle in the Econometrics models in estimating the prices based on the theories that estimate the interaction of buyers and sellers. The Random Walk Hypothesis, RWH, and the Efficient Market Hypothesis, EMH, are the leading theoretical models that describe such interactions [28]. Although the empirical models for identifying gold, and crude oil prices are efficient for accurate prediction, they are in some way complicated. Therefore, regression methods are utilized to deal with ambiguous relationships between various factors. In the regression-based methods, the parametric and non-parametric regression can be utilized [29]. Lately, the Autoregressive Integrated Moving Average, ARIMA, and Generalized Autoregressive Conditional Heteroskedasticity, GARCH, models have been utilized [11,12]. The parametric regression is efficient if there is Gaussian distribution for the values of the outcomes [30]. Otherwise, the nonparametric ones are more efficient [31]. Usually, the parametric methods are more powerful than nonparametric for datasets containing a small number of samples [32]. The regression-based model includes autoregression, and artificial intelligence-based methods. The Markov-switching vector is an example for autoregression, while the Artificial intelligence forecasting models include the artificial neural network (ANN) [33], Gaussian process regression (GPR) [34], and support vector machine (SVM) [35].

The oil/gold prices forecasting is challenging due to its nonlinear characteristics. Therefore, the research in this field never ends. For example, Yu et al. [36] have built a historical-based forecasting model for the oil prices during the period (1990–2008). They have used the SVM regressor and compared the performance to the ARIMA regressors. SVM has surpassed the ARIMA, but they cannot describe the nonlinear relationship of oil prices and ignore the relations of short-term influences. Another historical-based prediction is carried out in [37] using the classical ML regression techniques and the retrieved results were compared with the well-known regressor, ARIMA. The nonlinear characteristics of the oil/gold prices have been handled by utilizing the ANN regression models such as the work carried out by [12]. They have also built a historical-based regression model using the ANN approach and compared their performance with the linear methods including the ARIMA and GARCH methods during the period (1983 to 2003). Indranil et al. [38] have utilized the ANN, and LSTM [39] in enhancing an existing stochastic model for analyzing the commodity market, Barndorff-Nielsen, and Shephard model. The utilization of ML approaches in that stochastic model has handled its weak points such as the absence of long-term dependence between influencing factors.

The impact of input features being used in the training of the oil/gold forecasting models has been studied in few studies such as the work carried out in [20]. They have introduced filter, wrapper, and hybrid feature selection methods to detect the significant factors that may influence the accuracy of the prediction of the oil price. Linear regression, ANN, and SVM have been utilized in the training of forecasting models. The utilization of feature selection in that study facilitated the achievement of the outstanding performance for the forecasting models. The dimension reduction of the feature space has been introduced in [9] in forecasting the oil prices. The PCA along with locally linear embedding and the multidimensional scale as dimensional reduction techniques have been used and

compared. RNN, and LSTM as historical-based forecasting models have been employed in building the forecasting models.

The common conclusion among the aforementioned studies is that the forecasting of the crude oil and gold prices during the COVID-19 is demanding advanced forecasting models to overcome the nonlinearity of its characteristics. The promising results yielded using the ANN generally along with the increased accuracy observed using deep learning methods encourage this study to accomplish better accuracy using the feature extraction methodologies.

This study contributes the following:

- Analysis of recently published COVID-19 data sets along with the crude oil, and gold prices during that global health crisis and studying the impact of high spread and mortality rates, precautionary measures, and vaccinations on the prices of such commodities.
- Deep Autoencoders are integrated with the correlation analysis approach in selecting the key features that affect the accuracy of the forecasting models.
- The Bayesian regularization-backpropagation algorithm is utilized to avoid the overfitting of data which is a major drawback of training ANNs on the small-size datasets.

3. Methods

In this study, we have followed the framework depicted in Figure 1. The data set has been integrated from four public data sets including the COVID-19 records published by the Johns Hopkins University Center for Systems Science and Engineering web site [40], the World Daily Spot Prices for Crude Oil WTI, and Brent [41] published by King Abdullah Petroleum Studies and Research Center, the World Gold Council [42], and the indexes of the stock market directions from Yahoo Finance [43]. Five stock markets indexes have been utilized in this study including Vanguard Total Stock Market (VUN), Vanguard Total Stock Market Index Fund ETF Shares (VTI), Vanguard Value Index Fund ETF Shares (VTV), Emerging Markets Index (MME), and the Emerging Markets NTR Index (MMN). The integrated dataset has been preprocessed to impute the missing values and normalization. Then the data records have been divided randomly into training/testing samples with a percentage of 70/30%, respectively. The training samples are utilized to build the prediction models while the testing samples are employed to evaluate their prediction accuracy. The training/testing samples are then fed to a feature selection stage to select the key factors that may influence the prediction accuracy. We have conducted three different experiments to decide the optimum approach. In the first experiments, the relevant features have been extracted using the *PCC* are fed to neural networks regressor. The relevant features extracted using the correlation analysis are the ones that have higher Pearson Correlation Coefficient [44], with the outcomes. In the second experiment, the input variables are passed to a 2-stages stacked autoencoder deep network to extract a set of distinguishing latent features. The latent feature set is then fed to the regression model. Finally, in the third experiment, we have combined the *PCC* analysis with deep autoencoders. The relevant features extracted using the correlation analysis have been fed to the deep autoencoder to extract the latent features which are then submitted to the regression model. The fitting NN regressor that mapped the numeric input features to the numeric targets is two layers of feedforward NN with 10 sigmoid hidden neurons and linear transfer function in its output neurons. The NN has been trained using the Bayesian Regularization-backpropagation algorithm which can result in yielding a good generalization for small noisy datasets.

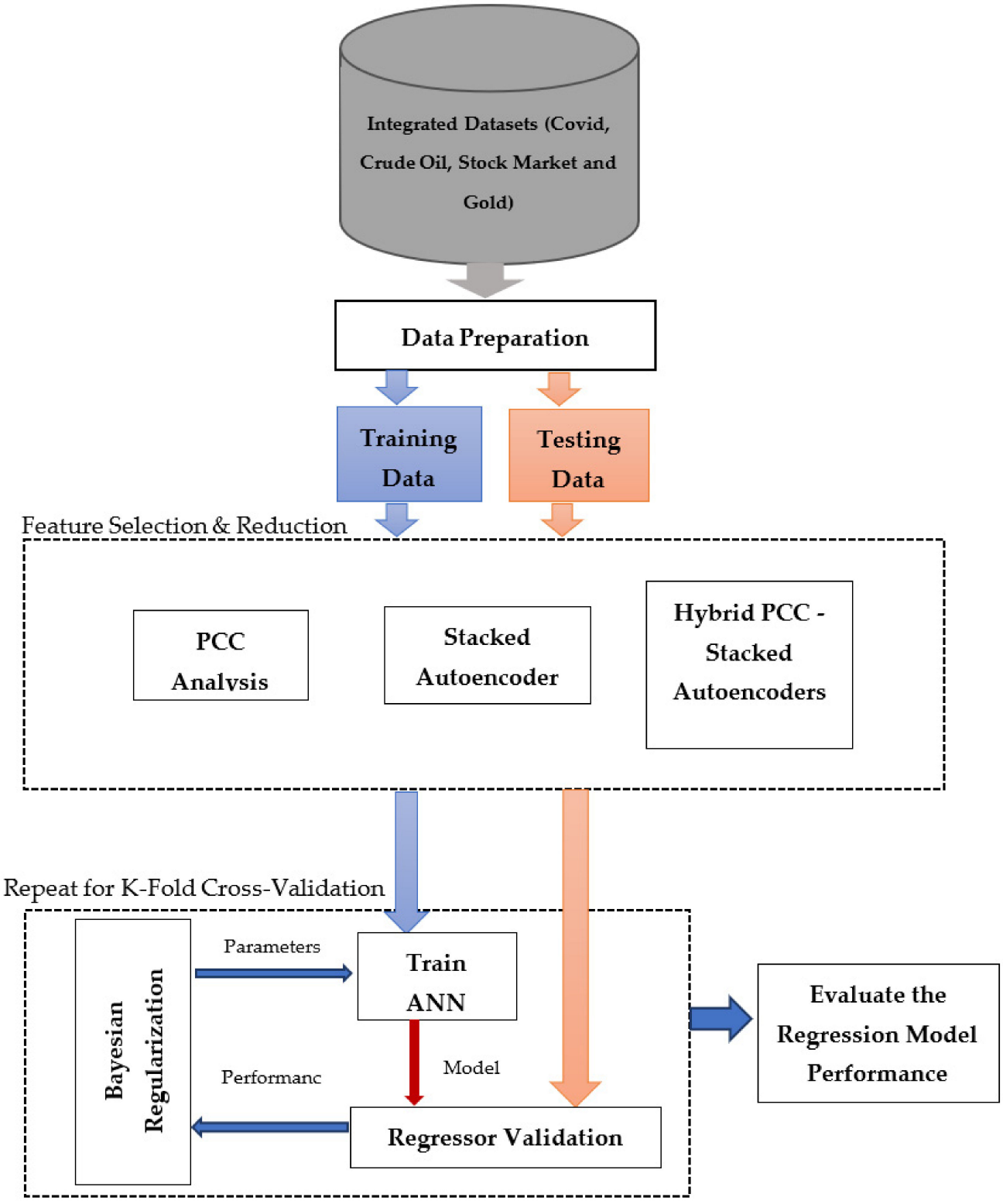

Figure 1. The framework of the proposed forecasting system for Gold, and Crude Oil prices.

3.1. Data Exploration and Hypothesis Testing

3.1.1. Data Exploration and Preprocessing

The COVID-19 data set records for Saudi Arabia have been downloaded starting from 1 April 2020 to the end of September 2021, along with the corresponding prices for crude oil, and gold in the same period. The Gold and oil datasets have several missing values because of market closures for weekends, and holidays. Therefore, the data values were padded to interpolate the values of the missing entries. The padding is preferred over other interpolation approaches as it is more insightful to refer to the final exchange rates and values as the current one. Additionally, there were two missing entries for the oil prices on 31 May 2021, and 30 August 2021, and they have been estimated by averaging the adjacent values. The COVID data contains 36 variables including the number of new confirmed cases, the total number of confirmed cases, new deaths, the total number of deaths, the total number of tests, and other supplementary entries. Lately, the published COVID data contained new variables that may influence the accuracy of the forecasting models including the Stringency index, reproduction rate, Positive Rate, and vaccinations. Stringency index is a composite measure of the precautionary measures based on various response indicators such as workplace closures, school closures, and travel bans. The values of the Stringency index range from 0 to 100, the value of 100 denotes the strictest policies. The reproduction rate of coronavirus gives an estimate of the possible extent of the virus transmission. The Positive Rate is an indicator of the Spread of the Virus. Based on the criteria announced by WHO in 2020, if the positive rate is less than 5% then the pandemic is under control in a country. The vaccination has been started in Saudi Arabia on 7 January 2021, therefore all previous values before this date have been set to zero. There were 43 missing values in the vaccinations field that have been imputed using the Growth Interpolation as depicted in Figure 2. The overall records in the data set are 540. Table 1 depicts a statistical description of the integrated dataset. The entries of Table 1 provide a summary of the distribution of the data values including the count represented by symbol N, the mean, standard deviation, the minimum, the 1st quantile, the mean, the 2nd quantile, and the maximum. The distribution of varying variables is illustrated by the aid of drawing the corresponding histogram as shown in Figure 3. The correlation matrix between all variables except those having zero variance is illustrated in Figure 4. The oils prices show a higher correlation with the variables describing the COVID-19 spread and the market prices than those for the gold prices.

Plots of the response variables versus the 540 days are shown in Figure 5. To prepare the integrated data records for the analysis, the entries have been normalized using the z-score approach. The normalized values are centralized around zero and have a standard deviation of one. For a random variable X having a mean value of μ and a standard deviation σ, the values of its *z-scores* are defined by Equation (1).

$$z\text{-}score = \frac{X - \mu}{\sigma} \tag{1}$$

There are several performance metrics to determine the loss in regression models including the Mean Square Error, *MSE*, and the R squared. All these metrics try to calculate the differences between the forecasted, and the actual values as depicted in Equation (2) where N, y_i, and $\hat{y}_i$ are the number of observations, the actual, and the predicted values, respectively.

$$MSE = \frac{1}{N}\sum_{i=1}^{N}(y_i - \hat{y}_i)^2 \tag{2}$$

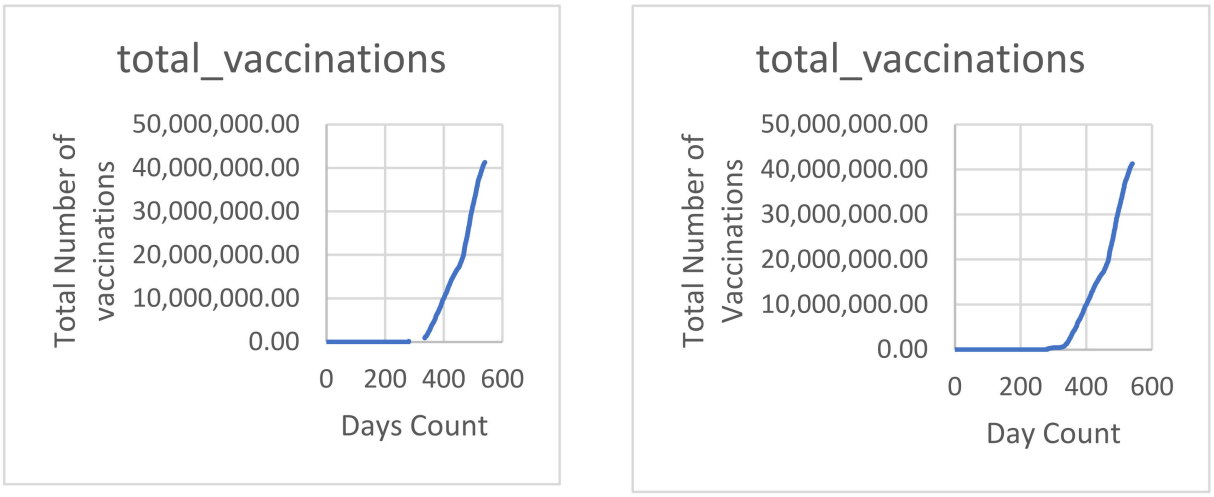

(**a**) (**b**)

Figure 2. Plots of the total number of vaccinations versus the day count (**a**) with the 43 missing data points, (**b**) after imputing the missing values using the Growth Interpolation technique.

Table 1. Statistical summary of the integrated dataset.

Variable	N	Mean	Std. Dev.	Min	Pctl. 25	Pctl. 75	Max
Days	540	270.5	156.029	1	135.75	405.25	540
TC	540	337,834.8	146,380.1	1720	295,556.3	427,619.8	546,735
NC	540	1009.578	1020.568	0	314.75	1287.5	5439
NC-smoothed	540	407.053	412.462	0	129.429	672.286	1403.857
TD	540	5189.746	2653.295	16	3329.25	7088.25	8679
ND	540	16.054	13.059	0	6	24	77
ND-smoothed	540	9.581	2.993	0	8.964	9.857	18.857
TC-per-million	540	14,022.01	1969.446	10,260.16	12201.24	15,470.42	15,470.42
NC-per-million	540	10.427	16.008	0	1.528	13.78	153.902
NC-smoothed-per-million	540	11.518	11.671	0	3.662	19.023	39.724
TD-per-million	540	226.089	25.436	175.831	201.779	245.581	245.581
ND-per-million	540	0.23	0.182	0	0.198	0.198	2.179
ND-smoothed-per-million	540	0.271	0.085	0	0.254	0.279	0.534
reproduction-rate	540	0.995	0.234	0.42	0.86	1.1	1.85
NT	540	52,740.05	24,304.74	6384	39,533.25	63,680.75	117620
TT	540	11,691511	8,474,141	123,706	4,308,481	17,687,639	28,595,954
TT-per-thousand	540	672.854	176.113	311.55	506.628	809.151	809.151
NT-per-thousand	540	1.662	0.486	0.769	1.461	1.665	3.328
NT-smoothed	540	57,632.22	17,104.68	31499	49661	58934	108916
NT-smoothed-per-thousand	540	1.631	0.484	0.891	1.405	1.668	3.082
positive-rate	540	0.029	0.042	0	0.007	0.021	0.194
tests-per-case	540	266.325	148.619	55.9	108.475	383.7	1029.2
total-vaccinations	540	6,862,518	11,437,967	0	0	10,809,238	41,290,665
stringency-index	540	60.142	12.783	50	52.78	60.19	94.44
VUN	540	66.722	7.722	47.36	60.58	72.465	80.3
VTI	540	199.288	27.629	122.38	175.482	221.49	234.31
VTV	540	124.528	15.734	84.78	107.958	138.33	142.41
MME	540	1236.719	149.344	807.4	1119.5	1341.4	1457.5
MMN	540	600.966	75.567	386.1	540.325	653.8	704.7
gold-price	540	6814.958	309.29	5919.95	6556.3	7053.407	7752.23
oil-prices	540	52.933	16.372	9.12	41.34	68.73	78.34

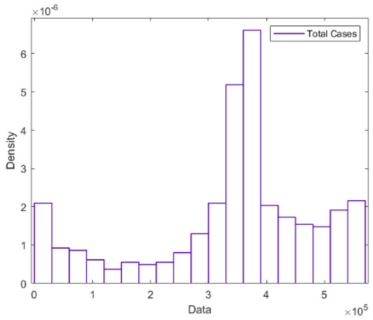

(1) Histogram of the total number of confirmed COVID-19 cases

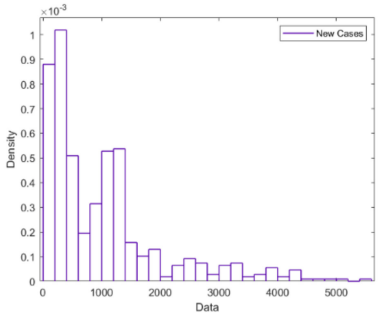

(2) Histogram of the total number of new COVID-19 cases

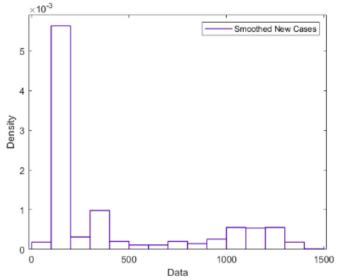

(3) Histogram of the smoothed total number of new COVID-19 cases

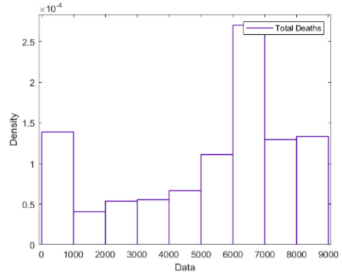

(4) Histogram of the total number of COVID-19 deaths

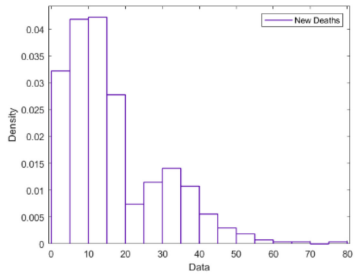

(5) The number of new COVID-19 deaths

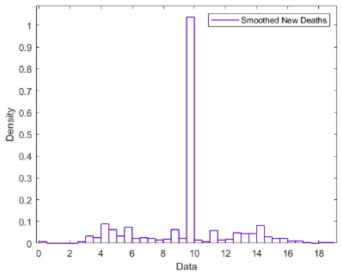

(6) The smoothed number of COVID-19 new deaths

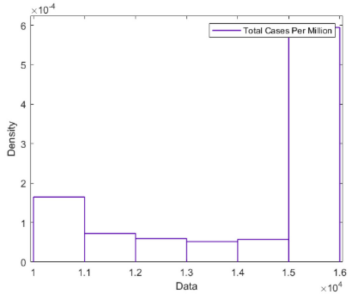

(7) The total number of COVID-19 cases per million

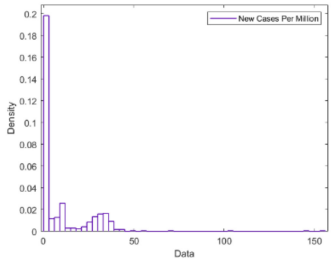

(8) The number of new COVID-19 cases per million

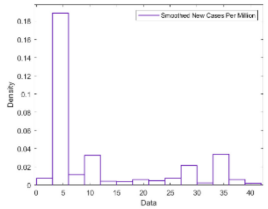

(9) The smoothed number of new COVID-19 cases per million

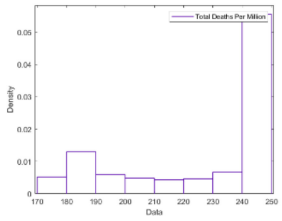

(10) The total number of COVID-19 deaths per million

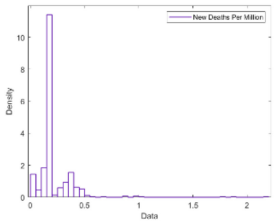

(11) The number of COVID-19 new deaths per million

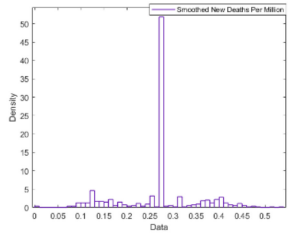

(12) The smoothed number of COVID-19 new deaths per million

Figure 3. *Cont.*

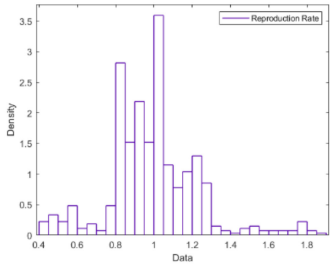

(13) The COVID-19 reproduction rate

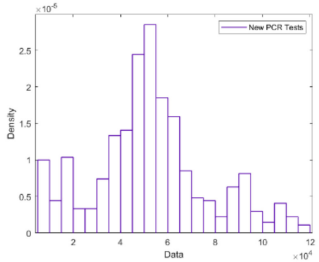

(14) The number of COVID-19 new PCR tests

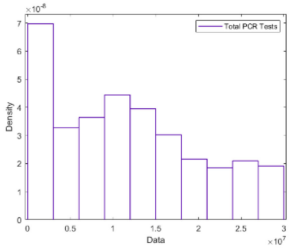

(15) The total number of COVID-19 PCR tests

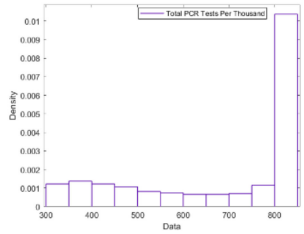

(16) The total number of COVID-19 PCR tests per thousands

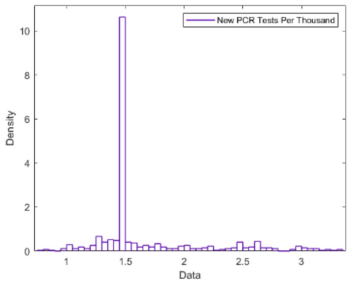

(17) The number of COVID-19 new PCR tests per thousands

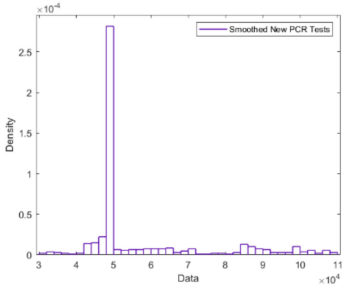

(18) The smoothed number of COVID-19 new PCR tests

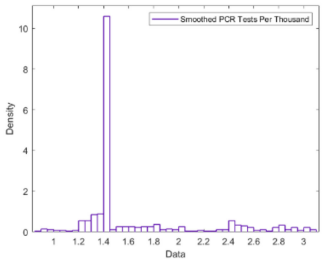

(19) The smoothed number of COVID-19 new PCR tests per thousands

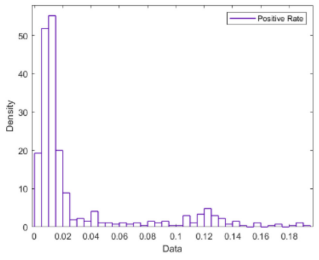

(20) The positive rate of the COVID-19 spread.

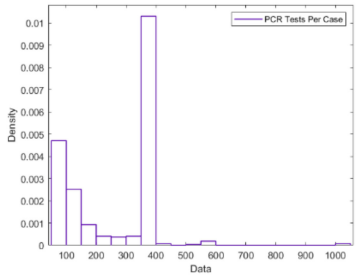

(21) The number of COVID-19 PCR tests per case

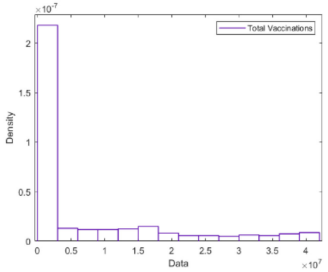

(22) The total number of COVID-19 vaccinated persons

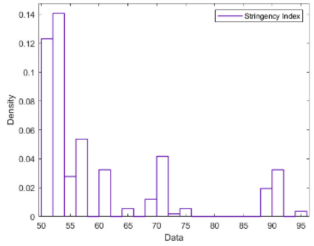

(23) The stringency index

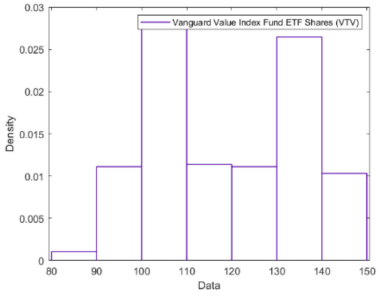

(24) The Vanguard Value Index Fund ETF Shares (VTV)

Figure 3. *Cont.*

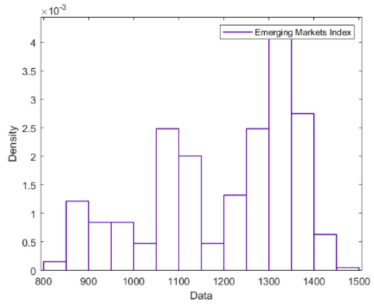

(25) The Emerging Markets Index

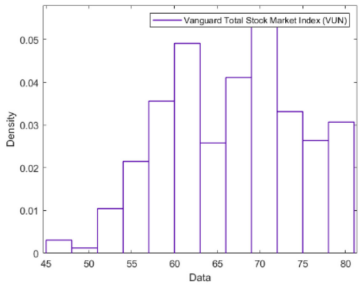

(26) The Vanguard Total Stock Market (VUN)

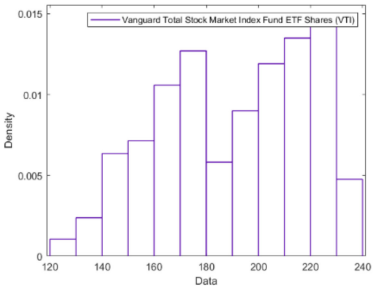

(27) The Vanguard Total Stock Market Index Fund ETF Shares (VTI)

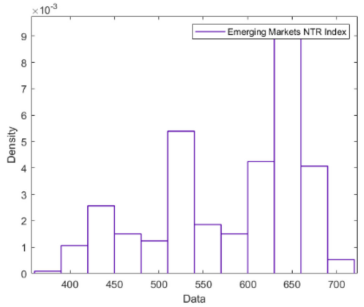

(28) The Emerging Markets NTR Index

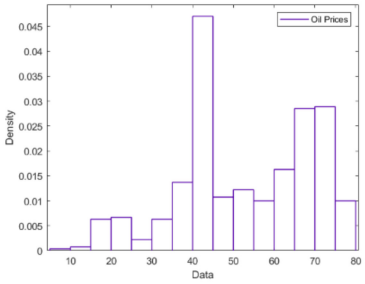

(29) Oil prices

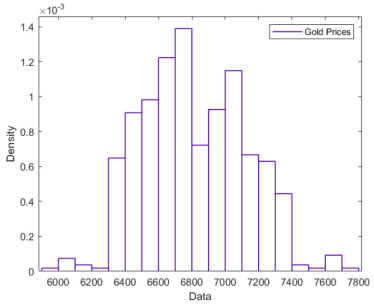

(30) Gold prices

Figure 3. Histograms of varying variables in the integrated dataset.

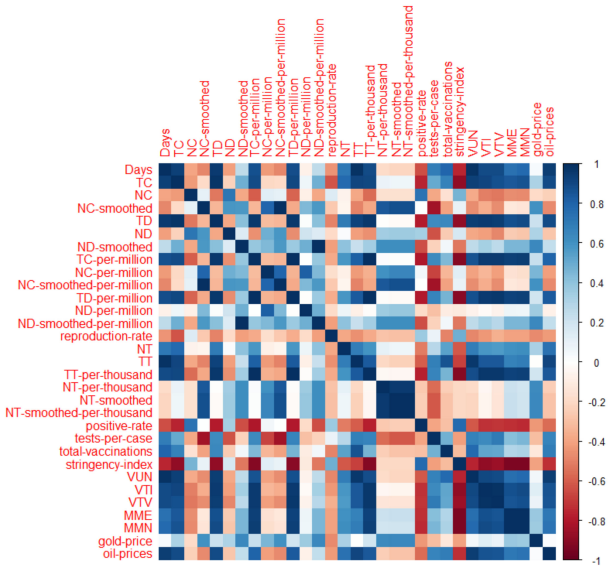

Figure 4. The correlation matrix of the integrated dataset (TC, NC, TD, ND, NT, and TT denotes Total Cases, New Cases, Total Deaths, New Deaths, New Tests, and Total Tests).

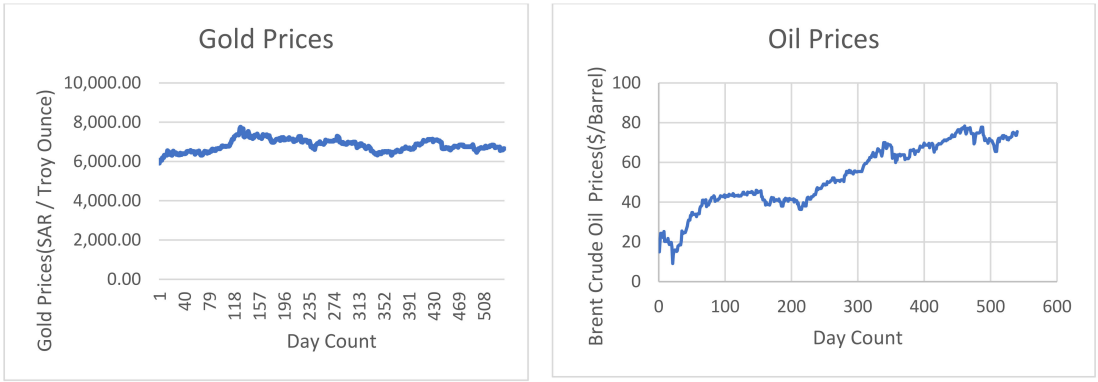

(**a**) (**b**)

Figure 5. Plots of the Gold/Oil prices versus 540 Days under the COVID-19 Pandemic; (**a**) Gold prices; (**b**) Oil prices.

3.1.2. Hypothesis Testing

To assess the validity of the proposed models in making good predictions for the prices of the oil, and gold prices during the COVID-19 pandemic, we have utilized the hypothesis testing for the whole population. In multiple linear regression, the null hypothesis in a population p can be formulated as $H_0 : \beta_1 = 0, \beta_2 = 0, \beta_3 = 0, \ldots \beta_p = 0$ which reveals that there is no relationship between the outcome and the p input predictors. The model is effective if there any $\beta \neq 0$ which is called the alternative hypothesis H_a where $H_a : \textit{at least one } \beta_j \neq 0 \ (j = 1, \ldots p)$. In this study, we have used the ANOVA F-statistics test as a way of hypothesis testing. We have excluded the variable that has zero variance from the test. In regression-based problems, the test is performed by measuring the significance level of the estimated coefficients yielded from linear regression models. The significance of each estimated coefficient is measured by calculating four metrics including the sum of squares (SS), the mean sum of squares (MS), the F-statistic, and the p-value. Table 2 displays the retrieved results of the test for the oil/gold prices. Based on the retrieved values of both the F-value, and the p-value, the null hypothesis must be rejected and it is revealed that there is a linear association between the outcomes (oil, and gold prices) and more than one of the input predictors in the integrated dataset.

Table 2. ANOVA test for the oil/gold prices and the input predictors.

Variable Symbol	Oil Prices				Gold Prices			
	SS	***MSE***	**F Value**	***p*-Value**	**SS**	***MSE***	**F Value**	***p*-Value**
TC	97.27	97.27	19.27	1.45×10^{-5}	27,824,836	27,824,836	1511	1.91×10^{-138}
NC	2879.85	2879.85	570.56	3.37×10^{-79}	211,353.5	211,353.5	11.48	0.0007
NC_smoothed	996.57	996.57	197.44	8.81×10^{-37}	129,593.1	129,593.1	7.039	0.008
TD	90.75	90.75	17.98	2.77×10^{-5}	6075.404	6075.404	0.33	0.565
ND	22.07	22.07	4.37	0.037	93.30752	93.30752	0.005	0.943
ND_smoothed	1229.91	1229.91	243.67	2.66×10^{-43}	230,428.2	230,428.2	12.51	0.0004
TC_per_million	1370.09	1370.09	271.44	5.38×10^{-47}	4677.894	4677.894	0.25	0.614
NC_per_million	0.54	0.54	0.11	0.743	542.2688	542.2688	0.029	0.863
NC_smoothed_per_million	32.67	32.67	6.47	0.011	7617.666	7617.666	0.41	0.520
TD_per_million	474.52	474.52	94.01	4.045×10^{-20}	150,517.9	150,517.9	8.17	0.004
ND_per_million	23.41	23.41	4.64	0.031	5520.553	5520.553	0.29	0.584
ND_smoothed_per_million	0.03	0.03	0.01	0.940	33,612.67	33,612.67	1.82	0.177
reproduction_rate	440.53	440.53	87.28	6.51×10^{-19}	149,960.9	149,960.9	8.146	0.004
NT	110.80	110.80	21.95	3.82×10^{-6}	686,444.9	686,444.9	37.29	2.397
TT	664.40	664.40	131.63	1.46×10^{-26}	6409.206	6409.206	0.34	0.555
TT_per_thousand	15.63	15.63	3.10	0.079	266,227.8	266,227.8	14.46	0.0001
NT_per_thousand	0.48	0.48	0.09	0.758	50,317.62	50,317.62	2.73	0.099
NT_smoothed	26.45	26.45	5.24	0.022	68,690.21	68,690.21	3.73	0.054
NT_smoothed_per_thousand	1.19	1.19	0.24	0.627	38,354.85	38,354.85	2.08	0.149
positive_rate	85.52	85.52	16.94	4.671×10^{-5}	10,960.87	10,960.87	0.59	0.44
tests_per_case	6.72	6.72	1.33	0.249	130,501	130,501	7.089	0.008
total_vaccinations	556.24	556.24	110.20	5.95×10^{-23}	1,404,073	1,404,073	76.27	6.66×10^{-17}
stringency_index	3.56	3.56	0.71	0.40	631,517.1	631,517.1	34.3	9.78×10^{-9}
VUN	4.68	4.68	0.93	0.33	4290.694	4290.694	0.23	0.629
VTI	9.56	9.56	1.89	0.169	1,256,655	1,256,655	68.26	2.08×10^{-15}
VTV	36.61	36.61	7.25	0.007	51,795.74	51,795.74	2.81	0.094
MME	31.10	31.10	6.16	0.013	1038.809	1038.809	0.05	0.81
MMN	19.89	19.89	3.94	0.0477	53,050.65	53,050.65	2.88	0.09
Gold_price	65.14	65.14	12.90	0.0003	237,554.9	237,554.9	12.9	0.0003

3.2. Pearson Correlation Coefficient Analysis

The Pearson Correlation Coefficient is an early method that finds the linear correlation between two random variables. *PCC* is a measure of similarity or dependency between two vectors. The *PCC* can be calculated for a pair of vectors X, and Y using Equation (3). Equation (4) represents the estimation for the *PCC*. If the input variables, X, and Y are correlated, the value of the *PCC* is between -1, and $+1$, linearly dependent. Otherwise, it is zero if they are uncorrelated.

$$PCC = \frac{cov(X,Y)}{\sqrt[2]{\sigma(X)\sigma(Y)}} \tag{3}$$

$$PCC = \frac{E(XY) - E(X)E(Y)}{\sqrt[2]{\sigma(X)\sigma(Y)}} \tag{4}$$

where, $E()$ is the expectation operator, $\sigma(X)$, and $\sigma(Y)$ are the variances of the variable X, and Y correspondingly, and $cov(X,Y)$ is the covariance matrix between them.

3.3. Stacked Deep Autoencoder

Autoencoder is a deep neural network used to learn a compressed representation of input data [22]. The autoencoder is trained to ignore insignificant data, noise, and its output is an encoding version for a set of data. This is the main idea in using the autoencoder for dimensional reduction of the feature space. The autoencoder comprises two modules including an encoder followed by a decoder [22]. The encoder module maps the input variables to a compressed form while the decoder tries to reverse the mapping to regenerate the input [22]. In this study, sparse autoencoders have been trained in an unsupervised manner using the Scaled Conjugate Gradient Algorithm, SCGA, [24] with 1000 training epochs. The autoencoder is used to extract the latent features and ignore the irrelevant ones. The input variables have been fed to the autoencoder and the number of neurons in the hidden layer has been adjusted to be less than the size of the input. We combined sparsity in the autoencoders by adding up a regularizer for the neurons' activations to the cost function [23]. As depicted in Equation (5), the cost function is the mean squared error function adjusted to contain two terms: the weight regularization, Ω_weights, and the sparsity regularization, Ω_sparsity [45]. The sparsity regularizer restricts the output from a neuron to be low allowing the autoencoder to discover a representation from a small portion of the training samples [23]. The weight regularization term avoids the values of the neuron weights from increasing which subsequently could reduce the sparsity regularizer. Equations (6) and (7) illustrate the mathematical representations of Ω_weights, and Ω_sparsity, respectively.

$$\begin{aligned} E = \underbrace{\frac{1}{M}\sum_{n=1}^{M}\sum_{k=1}^{N}(x_{kn} - \hat{x}_{kn})^2}_{mean\ squared\ error} \\ +\lambda \times \Omega_{weights} \\ +\beta \times \Omega_{sparsity} \end{aligned} \tag{5}$$

In Equation (3), M is a number of samples in the training subset, N is the number of input variables in the training data, x is a training sample, $\hat{x}$ is the estimate of the training sample, β, and λ are the coefficients of the sparsity, and weight regularizer, respectively [41].

$$\Omega_{weights} = \frac{1}{M}\sum_{l}^{L}\sum_{j}^{M}\sum_{i}^{K}\left(w_{ji}^{(l)}\right)^2 \tag{6}$$

In Equation (4), L represents the size of hidden layers, w is the weight matrix [41].

$$\Omega_{sparsity} = \sum_{i=1}^{D^{(1)}} KL\,(\rho \| \hat{\rho}_i) = \sum_{i=1}^{D^{(1)}} \rho\, log\left(\frac{\rho}{\hat{\rho}_i}\right) + (1-\rho)\, log\left(\frac{1-\rho}{1-\hat{\rho}_i}\right) \quad (7)$$

$$f(z) = \begin{cases} 0, & if\ z \leq 0 \\ z, & if\ 0 < z < 1 \\ 1, & if\ z \geq 1 \end{cases} \quad (8)$$

In Equation (5), $\hat{\rho}_i$ denotes the average activation of neuron i, while ρ represent the desired activation and, KL denotes the Kullback-Leibler divergence value between $\hat{\rho}_i$ and ρ [41].

As depicted in Figure 6, we have utilized a stacked autoencoders, 2 stages, beginning by training the first autoencoder, Autoencoder 1, on the input variables and using the extracted features from Autoencoder 1 as input to the second stage, Autoencoder 2. The transfer function used for the first encoder (Encoder 1) is the positive saturating linear transfer while the ordinary linear transfer function is used for the first decoder (Decoder 1). Positive saturating linear has been utilized in the encoder, and the decoder modules as depicted in Equation (8). We have set the learning parameters as shown in Table 3. In our experiment, all input variables: $M = 36$, $N = 540$ have been fed to Autoencoder 1. The number of extracted features from stage 1 was 10 features so the number of inputs to Autoencoder 2 have been as follows $M = 10$, $N = 540$. We have extracted 5 significant features from Autoencoder 2 and used them in the prediction phase. However, in experiment c, we have used the relevant features extracted by the correlation analysis, 22 features, as inputs to autoencoder 1. We have conducted many trials to set the values of all the learning parameters and the recorded values here are the ones that have yielded the minimum root mean squared error for the predicted values of the response variables.

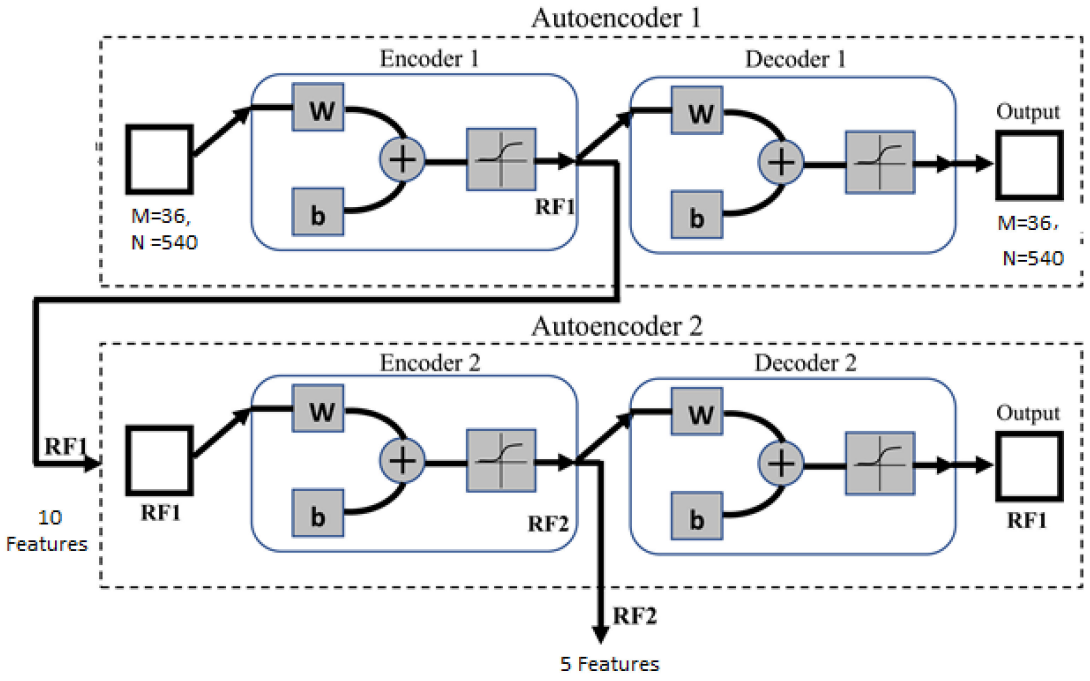

Figure 6. Two- Stages stacked deep autoencoder for Selecting Key features for Forecasting the oil, and gold prices.

Table 3. The values for the learning parameters used in the training of Autoencoder 1, and Autoencoder 2 in the stacked deep autoencoder.

Learning Parameters	Values
ρ (Sparsity Proportion)	0.05
β (Sparsity Regularization)	4
λ (coefficient of the weight regularizer)	0.002
No. of Epochs	1000

3.4. Bayesian Optimization for Regularization of NN Regressor

A common concern in estimating the weights of the NN is the overfitting in which the NN cannot generalize well and consequently, the performance on new data is inadequate. When overfitting happens, the weights are updated in a way that maximizes the accuracy of the training samples, but the NN fails on the testing data. The most common approach to resolving the overfitting is applying regularization in the estimation of network weights [46]. Regularization is employed to penalize the cost function, *MSE*, with the squared sum of the weights as illustrated by Equation (9).

$$E_{reg} = \gamma \sum_{k=1}^{l} \sum_{i,j=1}^{m} \left(w_{ij}^{k}\right)^2 + (1-\gamma)E = \gamma E_W + (1-\gamma)E \tag{9}$$

where γ is the regularization constant, E is the cost function (*MSE*), $k = 1, \ldots, l$ represents the network layers, and w_{ij}^{k} is the weights of neurons in layer k. The weights are estimated using the backpropagation algorithm which tries to minimize the cost function, E. The gradient descent algorithm is a conventional optimization algorithm for the estimation procedure. However, its performance is inadequate for small noisy datasets [23]. Bayesian regularization reduces the bias of the selection of the regularization constant and hence improves the performance. The objective function can be rewritten, as depicted in Equation (10), in terms of new hyperparameters α and β instead of γ.

$$F(W) = \alpha E_W + \beta E_D \tag{10}$$

where E_D is the sum of squared errors, $\sum_{i=1}^{N} \frac{1}{2}(y_i - \hat{y}_i)^2$.

The Bayesian optimization of the parameters of the regularization (α and β) can be summarized in the following steps [23]:

1. Initialize the weights, W, and the regularization parameters α, β.
2. Apply the Levenberg–Marquardt algorithm to minimize $F(W)$, the objective function.
3. Compute γ and k which are the effective, and a total number of parameters in the network $\gamma = k - 2\alpha tr H^{-1}$, where $H = 2\beta J^T J + 2\alpha I_k$ and J is the Jacobian matrix of the training errors.
4. Compute new estimation for the regularization parameters $\alpha = \gamma / 2E_W(W)$, and $\beta = (N - \gamma)/2E_D(W)$.
5. Repeat steps 2 to 4 until attaining convergence.

4. Results and Discussion

The main objective of this study is to investigate the impact of COVID-19 pandemic data in the forecasting models of gold, and oil prices. The basic idea is to select the most significant features that would yield an improved prediction accuracy. The NN regressor has been trained on 70% of the input data, 378 data samples, and tested on the remaining 30% of the data, 162 samples. Based on the attained results (F-value, and the p-value) from the hypothesis testing presented in Table 2, the null hypothesis that states that there is no relationship between the outcomes, oil/gold prices, and the integrated set of features have been rejected and a linear association between them has been considered. In addition,

the nonlinearity in such interactions can be detected via the deep autoencoder and the Bayesian-based NN regression model.

Figure 4 shows dark colors for the highly correlated features with the outcomes. In this study, only highly correlated features with the crude oil prices are considered relevant features. The retrieved values for the *PCC* of the gold prices and the input variables are much lower than those retrieved for oil prices. This ensures the higher sensitivity of the oil price to the COVID-19 pandemic, in contrast with the gold price. The gold is a shelter against economic crises and is believed as a safe haven during such health crises [47]. However, because it is well known that gold and oil prices have a strong association, the same set of selected features are used in their forecasting models. A further reduction for the relevant features has been made by selecting the features that have $PCC > \pm 0.7$ with the Oil prices based on the colored-based correlation matrix shown in Figure 4. The total number of vaccinations is highly correlated, $PCC = 0.713$, with the Oil prices and is influencing its prices. The vaccination has started almost after 300 days after the start of the pandemic in Saudi Arabia and has helped in the decreasing rate of the death rate and yielded a rapid increase in oil prices. However, the prices are still having up, and down variations with the emergence of the new strains of COVID-19.

We have selected the relevant features using a 2-stage stacked autoencoder as follows. The 36 features have been reduced into 10 features using the first stage and then a further reduction is carried out by the second stage of the autoencoder which yielded 5 significant features. A hybrid feature selection is carried out by applying the 2-stage stacked autoencoder on the features retrieved from the correlation analysis. Table 4 shows the retrieved values for the *MSE*, and R squared for the NN regressor on the testing samples when trained on all features, the significant ones retrieved by the *PCC* analysis, the Stacked autoencoder, and Hybrid method of the *PCC* analysis, and the SA for the oil, and gold, respectively. The corresponding fitting curves of the NN regression models are depicted in Figures 7 and 8, respectively. The hybrid method, *PCC*-Stacked Autoencoders, has yielded the minimum *MSE* and highest R squared values for the NN regressor as highlighted in gray color in Table 4. However, the autoencoder has yielded the worse performance when used solely on reducing the feature space as it fails to take into account the relationships of data features. The retrieved results using the hybrid method show that considering relationships in the data features can produce more robust features that can attain lower *MSE* in further regression compared to the other utilized methods. Figure 9 shows the predicted values versus the true ones for the gold and oil prices using the hybrid *PCC*-Stacked Autoencoders approach.

Table 4. The *MSE*, MAE, and R squared values for the NN regressor when trained on all features, the significant ones retrieved by the correlation analysis, the Stacked autoencoder, and Hybrid method for the oil, and gold, respectively.

	Oil Dataset			Gold Dataset		
Feature Selection Method	***MSE***	**MAE**	**R Squared**	***MSE***	**MAE**	**R Squared**
None	1.5×10^{-2}	0.0628	0.993	2.13×10^{-1}	0.2575	0.909
***PCC* Analysis**	1.23×10^{-2}	0.0583	0.994	1.13×10^{-1}	0.192	0.943
Stacked Autoencoders	2.019×10^{-2}	0.0865	0.989	2.357×10^{-1}	0.197	0.887
Hybrid *PCC*-Stacked Autoencoders	8.97×10^{-3}	0.0476	0.995	5.356×10^{-2}	0.0951	0.973

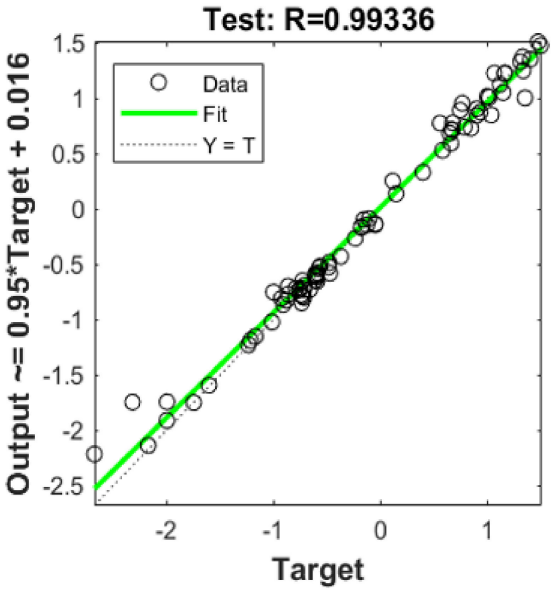

(**a**) All input features.

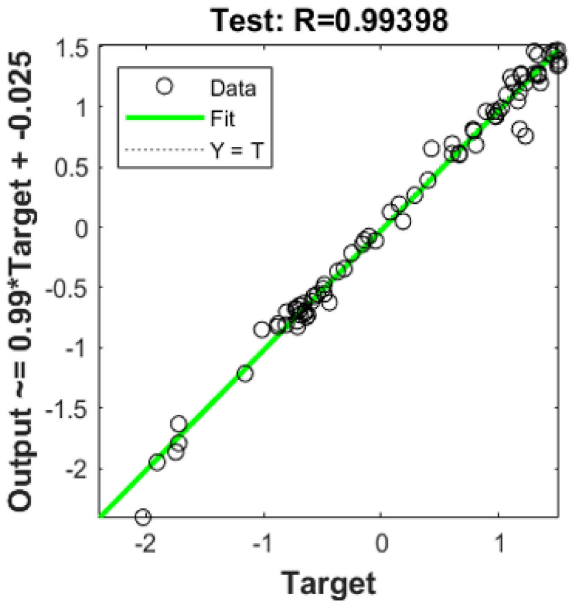

(**b**) *PCC*-features.

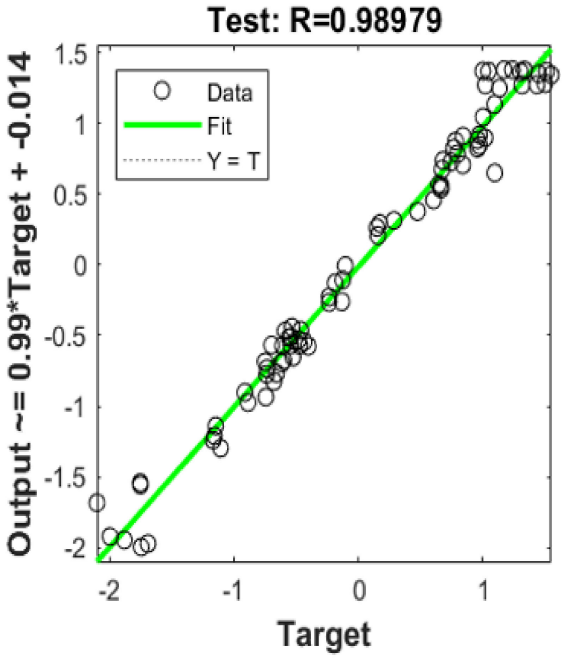

(**c**) Stacked Autoencoder features.

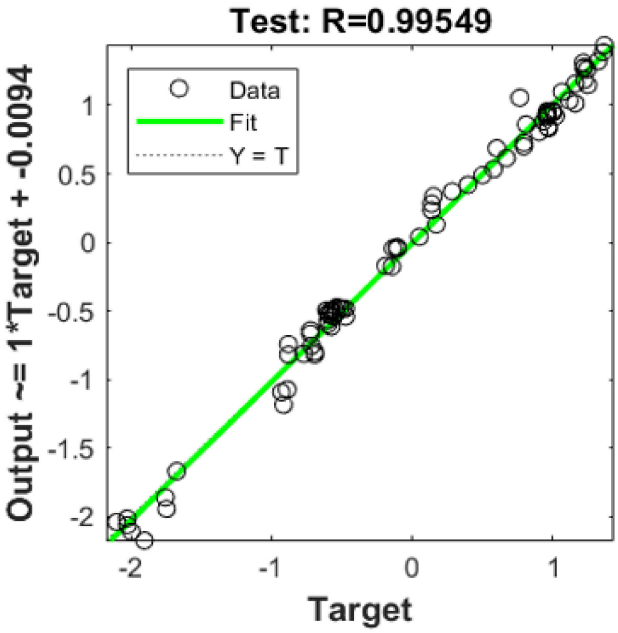

(**d**) *PCC*-Stacked Autoencoders feaures.

Figure 7. The fitting curve of the NN regression models trained using different sets of features for Oil Dataset.

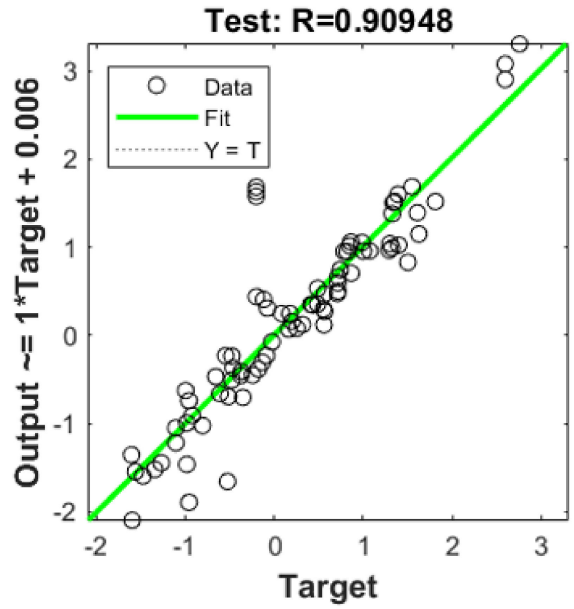

(**a**) All input features.

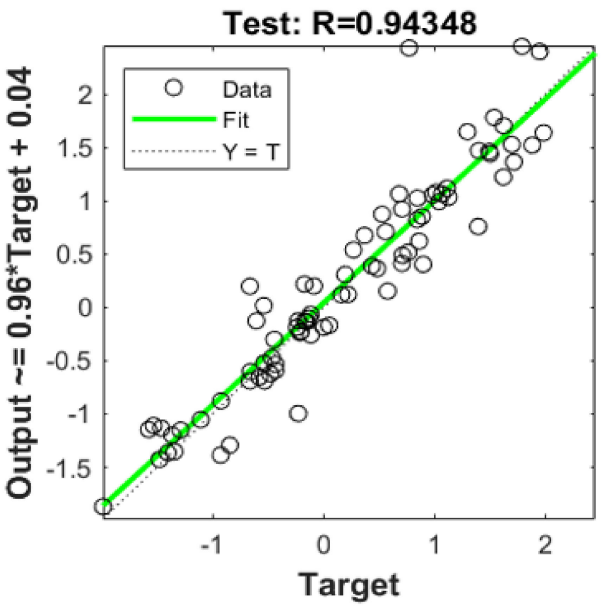

(**b**) *PCC*-features.

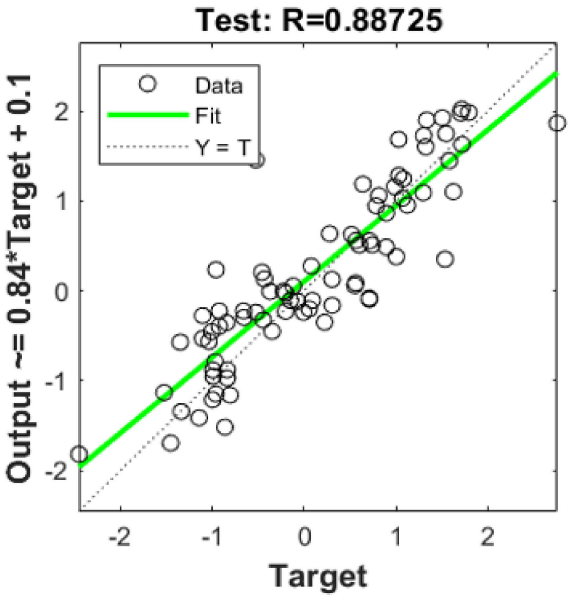

(**c**) Stacked Autoencoders features.

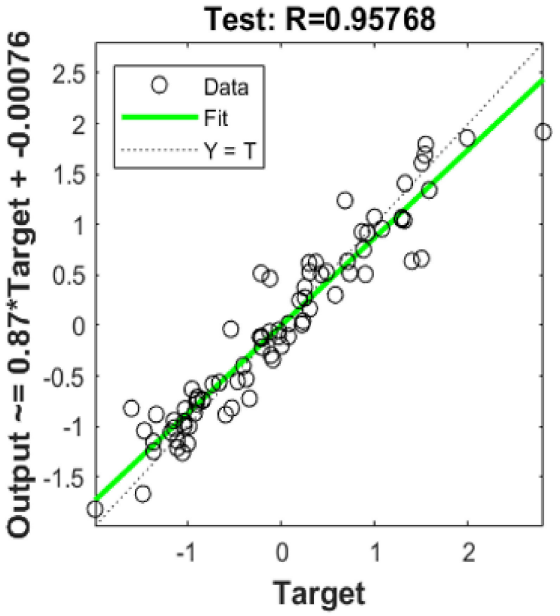

(**d**) *PCC*-Stacked Autoencoders features.

Figure 8. The fitting curves of the NN regression models trained using different sets of features for Gold Dataset.

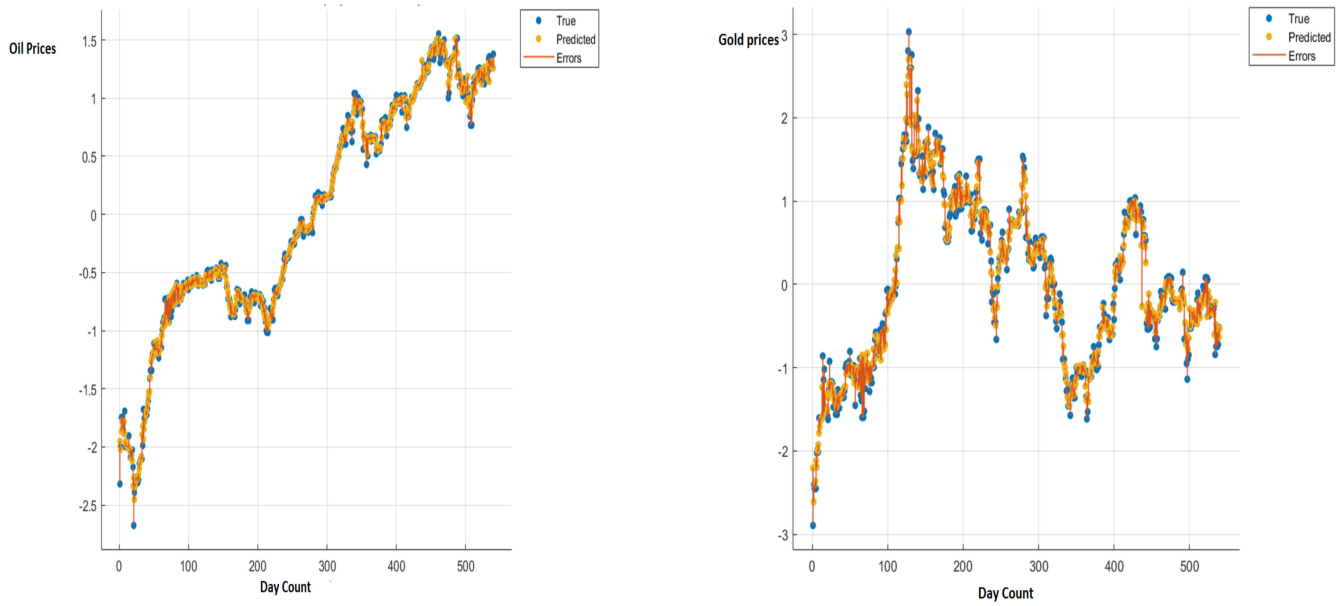

(**a**) Oil prices (**b**) Gold prices

Figure 9. The predicted values versus the true ones for the gold and oil prices versus 540 days during the COVID-19 pandemic using the hybrid feature extraction-based approach and NN regression models.

The performance of the proposed framework is evaluated versus several state-of-the-art forecasting models for oil, and gold prices. We compared our framework to that developed by Yu et al. [37], Xin James [48], Yan et al. [9], Weng et al. [49], He et al. [50], Khani et al. [51], and Jabeur et al. [52] as depicted in Table 5. The comparison shows that the proposed framework achieves the minimum RMSE, *MSE*, and MAE for forecasting the oil prices overall mentioned studies. The results yielded in this study have outperformed the early regression method, ARIMA, and the classical ML regressors including the SVR, and ANN. High performance has been attained by the help of using the proposed feature selection mechanism. In addition, we have compared our approach to another work [9] that has employed the feature reduction on the feature space of predicting the oil prices. They have retrieved 0.0844 for the MAE which is higher than the corresponding value yielded in our approach, 0.0476. Regarding the retrieved results for forecasting the gold prices, it has surpassed the ones yielded by the Multivariate Empirical Mode Decomposition approach [50] and is comparable with the attained results by Khani et al. [51]. The study of Yan et al. [9] in particular, was picked for comparison as it is very close to our proposed framework so far. Both studies similarly have utilized feature reduction approaches for selecting the significant features for building the forecasting models. However, Yan's study was applied only on oil datasets and used different methods rather than the deep autoencoder for the reduction of the feature space including the principal component analysis, PCA, locally linear embedding, LLE, and multidimensional scale, MDS.

Table 5. Comparing the results of the proposed framework for forecasting the oil, and gold prices with state-of the-art forecasting models.

Publication	Method	Dataset	*MSE*	R Squared	MAE	RMSE
Yu et al. [37]	Support Vector Regression (SVR), ANN, and ARIMA	Crude Oil	-	-	-	5.0493(ARIMA) 3.9337(SVR) 4.8682(ANN)
Xin James [48]	SVR, and ARIMA	Crude Oil prices	-	-	1.1433(ARIMA) 1.1246(SVR)	-
Yan et al. [9]	De-dimension machine learning model using PCA, and RNN/LSTM approach to forecast the oil prices.	Crude Oil prices	-	-	0.0844(RNN) 0.0905 (LSTM) 0.2784 (SVM)	-
Weng et al. [49]	Gold prices prediction using GA-ROSELM, genetic algorithm regularization online extreme learning machine	silver price, oil price, gold price	-	-	5.681	-
He et al. [50]	Denoising model to detect the noise factors in forecasting metal price using Multivariate Empirical Mode Decomposition	Silver, and gold prices	1.222	-	-	1.105
Khani et al. [51]	Encoder–decoder LSTM model for forecasting gold prices during the COVID-19 pandemic.	COVID-19 data records, and gold prices	0.0217	0.858	-	0.147
Jabeur et al. [52]	XGBoost machine learning approach for forecasting gold prices.	Metals, oil, and gold prices	-	0.994	21.948	-
Proposed framework	*PCC*-Stacked Autoencoder Hybrid feature extraction approach for forecasting the oil, and gold prices during the COVID-19 pandemic.	COVID-19 data records, oil, and gold prices	0.0089 (oil) 0.0536 (gold)	0.995 (oil) 0.973 (gold)	0.0476 (oil) 0.0951 (gold)	0.094 (oil) 0.231 (gold)

5. Conclusions

The global lockdown carried out with respect to the COVID-19 pandemic has severe consequences on the economy of the whole world. Oil and gold as well as experienced a downward trend due to the increased rate in the number of confirmed COVID-19 cases. Therefore, accurate forecasting for the oil, and gold during the COVID-19 period may assist the investors and stakeholders in their risk management decisions.

This study is the first one to investigate the impact of the lately published features of COVID-19 datasets that may influence the accuracy of the oil/gold prices forecasting models including the Stringency index, reproduction rate, Positive Rate, and Vaccinations. Based on the *PCC* analysis, the total number of vaccinations is positively correlated, *PCC* = 0.713, with the Oil prices and is strongly influencing its prices. The vaccination has aided in a rapid increase in oil prices. However, the developments of the new strains of COVID-19 are causing the instability of its prices. The yielded results provide an indication that the gold prices are more stable and have less sensitivity compared to the oil. The gold tends to respond in contrast with the other kinds of commodities which are highly affected with respect to the COVID-19 pandemic.

Deep autoencoders along with a Bayesian NN regressor are adopted to investigate the impact of COVID-19 pandemic datasets on gold/oil prices during the period 1 April 2020–30 September 2021 in Saudi Arabia. The key factors in the feature space that may influence the accuracy of the forecasting models are selected using a hybrid approach of stacked autoencoders and the Pearson Correlation analysis. The applied feature reduction methods including *PCC*, 2-stage Stacked Autoencoder, and the *PCC*-Stacked Autoencoders demonstrate that the hybrid approach has yielded more significant features by considering the relationship between the input features using the *PCC*. These key features have attained the minimum *MSE*, and highest R squared values for the NN regressor compared to other methods. The presented approach for forecasting the oil/gold prices has outperformed the early well-known regression technique, ARIMA, the classical ML (SVR, and ANN), and deep learning methods (RNN, and LSTM).

Author Contributions: Conceptualization, N.A.S. and G.A.; methodology, N.A.S., G.A., R.A., A.A.A. and H.N.A.; software, N.A.S. and G.A.; validation, N.A.S. and G.A.; formal analysis, N.A.S., G.A., R.A., A.A.A. and H.N.A.; investigation, N.A.S., G.A., R.A., A.A.A. and H.N.A.; resources, N.A.S.; data curation, N.A.S.; writing—original draft preparation, N.A.S., G.A., R.A., A.A.A. and H.N.A.; writing—review and editing, N.A.S., G.A., R.A., A.A.A. and H.N.A.; visualization, N.A.S.; supervision, H.N.A.; project administration, R.A.; funding acquisition, R.A. All authors have read and agreed to the published version of the manuscript.

Funding: This research was funded by Princess Nourah bint Abdulrahman University Researchers Supporting Project number (PNURSP2022R323), Princess Nourah bint Abdulrahman University, Riyadh, Saudi Arabia.

Acknowledgments: The authors express their gratitude to Princess Nourah bint Abdulrahman University Researchers Supporting Project number (PNURSP2022R323), Princess Nourah bint Abdulrahman University, Riyadh, Saudi Arabia.

Conflicts of Interest: The authors declare no conflict of interest.

References

1. Singleton, K.J. Investor Flows and the 2008 Boom/Bust in Oil Prices. *Manag. Sci.* **2014**, *60*, 300–318. [CrossRef]
2. Bernanke, B.S. Irreversibility, Uncertainty, and Cyclical Investment. *Q. J. Econ.* **1983**, *98*, 85. [CrossRef]
3. Soytas, U.; Sari, R.; Hammoudeh, S.; Hacihasanoglu, E. World Oil Prices, Precious Metal Prices and Macroeconomy in Turkey. *Energy Policy* **2009**, *37*, 5557–5566. [CrossRef]
4. Baur, D.G.; Lucey, B.M. Is Gold a Hedge or a Safe Haven? An Analysis of Stocks, Bonds and Gold. *Financ. Rev.* **2010**, *45*, 217–229. [CrossRef]
5. Mensi, W.; Reboredo, J.C.; Ugolini, A. Price-Switching Spillovers between Gold, Oil, and Stock Markets: Evidence from the USA and China during the COVID-19 Pandemic. *Resour. Policy* **2021**, *73*, 102217. [CrossRef]

6. Nicola, M.; Alsafi, Z.; Sohrabi, C.; Kerwan, A.; Al-Jabir, A.; Iosifidis, C.; Agha, M.; Agha, R. The Socio-Economic Implications of the Coronavirus Pandemic (COVID-19): A Review. *Int. J. Surg.* **2020**, *78*, 185–193. [CrossRef]
7. Bakas, D.; Triantafyllou, A. Commodity Price Volatility and the Economic Uncertainty of Pandemics. *Econ. Lett.* **2020**, *193*, 109283. [CrossRef]
8. Sharif, A.; Aloui, C.; Yarovaya, L. COVID-19 Pandemic, Oil Prices, Stock Market, Geopolitical Risk and Policy Uncertainty Nexus in the US Economy: Fresh Evidence from the Wavelet-Based Approach. *Int. Rev. Financ. Anal.* **2020**, *70*, 101496. [CrossRef]
9. Yan, L.; Zhu, Y.; Wang, H. Selection of Machine Learning Models for Oil Price Forecasting: Based on the Dual Attributes of Oil. *Discret. Dyn. Nat. Soc.* **2021**, *2021*, 1–16. [CrossRef]
10. Arfaoui, M.; ben Rejeb, A. Oil, Gold, US Dollar and Stock Market Interdependencies: A Global Analytical Insight. *Eur. J. Manag. Bus. Econ.* **2017**, *26*, 278–293. [CrossRef]
11. Zhang, Y.; Hamori, S. Forecasting Crude Oil Market Crashes Using Machine Learning Technologies. *Energies* **2020**, *13*, 2440. [CrossRef]
12. Moshiri, S.; Foroutan, F. Forecasting Nonlinear Crude Oil Futures Prices. *Energy J.* **2006**, *27*, 81–95. [CrossRef]
13. Zhang, J.L.; Zhang, Y.J.; Zhang, L. A Novel Hybrid Method for Crude Oil Price Forecasting. *Energy Econ.* **2015**, *49*, 649–659. [CrossRef]
14. Kristjanpoller, R.W.; Hernández, P.E. Volatility of Main Metals Forecasted by a Hybrid ANN-GARCH Model with Regressors. *Expert Syst. Appl.* **2017**, *84*, 290–300. [CrossRef]
15. Abdullah, S.N.; Zeng, X. Machine Learning Approach for Crude Oil Price Prediction with Artificial Neural Networks-Quantitative (ANN-Q) Model. In Proceedings of the International Joint Conference on Neural Networks, Barcelona, Spain, 18–23 July 2010. [CrossRef]
16. Wu, Y.X.; Wu, Q.B.; Zhu, J.Q. Improved EEMD-Based Crude Oil Price Forecasting Using LSTM Networks. *Phys. Stat. Mech. Appl.* **2019**, *516*, 114–124. [CrossRef]
17. Cen, Z.; Wang, J. Crude Oil Price Prediction Model with Long Short Term Memory Deep Learning Based on Prior Knowledge Data Transfer. *Energy* **2019**, *169*, 160–171. [CrossRef]
18. Kim, H.Y.; Won, C.H. Forecasting the Volatility of Stock Price Index: A Hybrid Model Integrating LSTM with Multiple GARCH-Type Models. *Expert Syst. Appl.* **2018**, *103*, 25–37. [CrossRef]
19. Rapach, D.E.; Zhou, G. Time-series and Cross-sectional Stock Return Forecasting: New Machine Learning Methods. In *Machine Learning for Asset Management*; Wiley: Hoboken, NJ, USA, 2020; pp. 1–33.
20. Wang, J.; Zhou, H.; Hong, T.; Li, X.; Wang, S. A Multi-Granularity Heterogeneous Combination Approach to Crude Oil Price Forecasting. *Energy Econ.* **2020**, *91*, 104790. [CrossRef]
21. Chen, Y.; He, K.; Tso, G.K.F. Forecasting Crude Oil Prices: A Deep Learning Based Model. *Procedia Comput. Sci.* **2017**, *122*, 300–307. [CrossRef]
22. Bashiri Behmiri, N.; Pires Manso, J.R. Crude Oil Price Forecasting Techniques: A Comprehensive Review of Literature. *SSRN Electron. J.* **2013**, 1–32. [CrossRef]
23. Sariev, E.; Germano, G. Bayesian Regularized Artificial Neural Networks for the Estimation of the Probability of Default. *Quant. Financ.* **2020**, *20*, 311–328. [CrossRef]
24. Osman, H.; Ghafari, M.; Nierstrasz, O. The Impact of Feature Selection on Predicting the Number of Bugs. *arXiv* **2018**, arXiv:1807.04486.
25. Javed, F.; Thomas, I.; Memedi, M. A Comparison of Feature Selection Methods When Using Motion Sensors Data: A Case Study in Parkinson's Disease. In Proceedings of the Annual International Conference of the IEEE Engineering in Medicine and Biology Society, Honolulu, HI, USA, 18–21 July 2018; Volume 2018, pp. 5426–5429. [CrossRef]
26. Atteia, G.; Abdel Samee, N.; Zohair Hassan, H. DFTSA-Net: Deep Feature Transfer-Based Stacked Autoencoder Network for DME Diagnosis. *Entropy* **2021**, *23*, 1251. [CrossRef] [PubMed]
27. Shamshirband, S.; Mosavi, A.; Rabczuk, T.; Nabipour, N.; Chau, K. Prediction of Significant Wave Height; Comparison between Nested Grid Numerical Model, and Machine Learning Models of Artificial Neural Networks, Extreme Learning and Support Vector Machines. *Eng. Appl. Comput. Fluid Mech.* **2020**, *14*, 805–817. [CrossRef]
28. Samuelson, P.A. Proof That Properly Discounted Present Values of Assets Vibrate Randomly. *Bell J. Econ. Manag. Sci.* **1973**, *4*, 369. [CrossRef]
29. Atteia, G.E.; Mengash, H.A.; Samee, N.A. Evaluation of Using Parametric and Non-Parametric Machine Learning Algorithms for COVID-19 Forecasting. *Int. J. Adv. Comput. Sci. Appl.* **2021**, *12*, 647–657. [CrossRef]
30. Smalheiser, N.R. Data Literacy: How to Make Your Experiments Robust and Reproducible. In *Data Literacy: How to Make Your Experiments Robust and Reproducible*; Academic Press: Cambridge, MA, USA, 2017; pp. 1–282. [CrossRef]
31. Arai, K. Combined Non-Parametric and Parametric Classification Method Depending on Normality of PDF of Training Samples. *Int. J. Adv. Comput. Sci. Appl.* **2021**, *12*, 310–316. [CrossRef]
32. Chin, R.; Lee, B.Y. *Principles and Practice of Clinical Trial Medicine*; Elsevier: Amsterdam, The Netherlands, 2008. [CrossRef]
33. Oh, J.; Suh, K.D. Real-Time Forecasting of Wave Heights Using EOF—Wavelet—Neural Network Hybrid Model. *Ocean Eng.* **2018**, *150*, 48–59. [CrossRef]

34. Li, Y.; Bao, T.; Chen, Z.; Gao, Z.; Shu, X.; Zhang, K. A Missing Sensor Measurement Data Reconstruction Framework Powered by Multi-Task Gaussian Process Regression for Dam Structural Health Monitoring Systems. *Measurement* **2021**, *186*, 110085. [CrossRef]
35. Hu, J.; Wang, J.; Ma, K. A Hybrid Technique for Short-Term Wind Speed Prediction. *Energy* **2015**, *81*, 563–574. [CrossRef]
36. Yu, L.; Zhang, X.; Wang, S. Assessing Potentiality of Support Vector Machine Method in Crude Oil Price Forecasting. *Eurasia J. Math. Sci. Technol. Educ.* **2017**, *13*, 7893–7904. [CrossRef]
37. Zhao, C.L.; Wang, B. Forecasting Crude Oil Price with an Autoregressive Integrated Moving Average (ARIMA) Model. *Adv. Intell. Syst. Comput.* **2014**, *211*, 275–286. [CrossRef]
38. SenGupta, I.; Nganje, W.; Hanson, E. Refinements of Barndorff-Nielsen and Shephard Model: An Analysis of Crude Oil Price with Machine Learning. *Ann. Data Sci.* **2021**, *8*, 39–55. [CrossRef]
39. Gers, F.A.; Schmidhuber, J.; Cummins, F. Learning to Forget: Continual Prediction with LSTM. *Neural Comput.* **2000**, *12*, 2451–2471. [CrossRef]
40. Johns Hopkins University Center for Systems Science and Engineering at JHU. Available online: https://coronavirus.jhu.edu/ (accessed on 10 February 2022).
41. World Daily Spot Prices for Crude Oil WTI and Brent—KAPSARC Data Portal. Available online: https://datasource.kapsarc.org (accessed on 16 January 2022).
42. Gold Price Historical Data | Gold Price History | World Gold Council. Available online: https://www.gold.org/goldhub/data/gold-prices (accessed on 16 January 2022).
43. Yahoo Finance—Stock Market Live, Quotes, Business & Finance News. Available online: https://finance.yahoo.com/ (accessed on 14 March 2022).
44. Boslaugh, S. The Pearson Correlation Coefficient. In *Statistics in a Nutshell*, 2nd ed.; O'Reilly Media Inc.: Sebastopol, CA, USA, 2012; pp. 80–92, ISBN 9781449316822.
45. Olshausen, B.A.; Field, D.J. Sparse Coding with an Overcomplete Basis Set: A Strategy Employed by V1? *Vis. Res.* **1997**, *37*, 3311–3325. [CrossRef]
46. Smirnov, E.A.; Timoshenko, D.M.; Andrianov, S.N. Comparison of Regularization Methods for ImageNet Classification with Deep Convolutional Neural Networks. *AASRI Procedia* **2014**, *6*, 89–94. [CrossRef]
47. Atri, H.; Kouki, S.; Gallali, M. imen The Impact of COVID-19 News, Panic and Media Coverage on the Oil and Gold Prices: An ARDL Approach. *Resour. Policy* **2021**, *72*, 102061. [CrossRef]
48. He, X.J. Crude Oil Prices Forecasting: Time Series vs. SVR Models. *J. Int. Technol. Inf. Manag.* **2018**, *27*, 25–42.
49. Weng, F.; Chen, Y.; Wang, Z.; Hou, M.; Luo, J.; Tian, Z. Gold Price Forecasting Research Based on an Improved Online Extreme Learning Machine Algorithm. *J. Ambient. Intell. Humaniz. Comput.* **2020**, *11*, 4101–4111. [CrossRef]
50. He, K.; Chen, Y.; Tso, G.K.F. Price Forecasting in the Precious Metal Market: A Multivariate EMD Denoising Approach. *Resour. Policy* **2017**, *54*, 9–24. [CrossRef]
51. Mohtasham Khani, M.; Vahidnia, S.; Abbasi, A. A Deep Learning-Based Method for Forecasting Gold Price with Respect to Pandemics. *SN Comput. Sci.* **2021**, *2*, 335. [CrossRef] [PubMed]
52. Jabeur, S.B.; Mefteh-Wali, S.; Viviani, J.L. Forecasting Gold Price with the XGBoost Algorithm and SHAP Interaction Values. *Ann. Oper. Res.* **2021**, *937*, 1–21. [CrossRef]